

# Thermal Desorption Induced by Kilolectronvolt Ion Bombardment of Thiol-Bound Self-Assembled Monolayers on Gold

D. E. Riederer,<sup>†</sup> R. Chatterjee, S. W. Rosencrance,<sup>‡</sup> Z. Postawa,<sup>§</sup> T. D. Dunbar, D. L. Allara, and N. Winograd\*

Contribution from the Department of Chemistry, 184 Materials Research Institute Building, The Pennsylvania State University, University Park, Pennsylvania 16802-7003

Received April 7, 1997<sup>⊗</sup>

**Abstract:** Time distributions of neutral molecules desorbed from a chemisorbed self-assembled monolayer of phenylethanethiol on gold have been measured subsequent to 8 keV Ar<sup>+</sup> and H<sub>2</sub><sup>+</sup> ion bombardment. These distributions show that, regardless of the projectile used, most of the ejected molecules leave the surface with thermal kinetic energies (~0.03 eV). The shapes of the distributions have a strong surface temperature dependence over the range 240–300 K. This behavior is well described by a convolution of the Maxwell–Boltzmann distribution and the rate equation for first-order desorption. The results imply that kilolectronvolt ion bombardment initiates a process which breaks the adsorbate–surface bond, leaving the resulting physisorbed molecules to evaporate after attaining thermal equilibrium with the substrate. A mechanism for this gentle cleavage of the adsorbate–substrate bond is proposed.

## Introduction

There has been much recent interest in surfaces bearing covalently bound molecules. Examples of such surfaces include self-assembled monolayers on metal substrates,<sup>1,2</sup> and a variety of molecules bound to polystyrene spheres.<sup>3</sup> These thin molecular films vary in thickness from ten to a few hundred angstroms and may be tailored to have desired physical and chemical properties. Molecular surfaces of this type are used to control both wetting properties<sup>4</sup> and biological compatibility.<sup>5</sup> They are also used extensively in combinatorial synthesis and in the immobilization of biomolecules on surfaces.<sup>6–8</sup> Although mass spectrometric techniques have been among the most powerful in characterizing these types of materials, the presence of the covalent bond often makes the analysis difficult without first chemically releasing the target molecule by clipping at the attachment site.

Energetic probes, such as fast particles<sup>9–12</sup> and photons,<sup>13</sup> play a central role in the characterization of molecular solids.

Understanding events which lead to molecular desorption is important since methods utilizing these probes are rapidly expanding as a means for chemically mapping complex surfaces.<sup>14–16</sup> There is a great deal of qualitative information about the mechanisms by which molecules desorb, although so far it is difficult to make *a priori* predictions regarding the behavior of individual systems. Such predictions require a fundamental understanding of how the events initiated by energetic probes lead to the eventual ejection of molecular species from the surface.

In the present work, the time distributions of neutral molecules or fragments desorbed from a self-assembled monolayer of phenylethanethiol on gold upon pulsed kilolectronvolt ion bombardment are reported. Translational energies and desorption delay times obtained from these measurements provide elementary information about neutral molecule desorption which is decoupled from the ionization processes. The time dependence of the desorption event was obtained by measuring the time between a pulsed ion/surface collision and the arrival of desorbed neutral molecules at a photon field located a fixed distance above the surface. The results strongly implicate the operation of a two-step desorption mechanism which involves gentle cleavage of a covalent bond in a manner which enables the nascent species to remain trapped at the surface. This is followed by evaporation of the thermally equilibrated, physisorbed molecule. A mechanism for the gentle cleavage of a bond within the surface linkage is proposed. It is suggested that, at least for certain systems, covalently bound molecules may be cleanly removed from their binding support. These findings are particularly relevant to the direct chemical assay of covalently bound surface molecules.<sup>17</sup>

<sup>†</sup> Permanent address: Department of Chemistry, University of Missouri, Columbia, MO 65211.

<sup>‡</sup> Permanent address: Corporate Research and Development, NALCO Chemical Co., One NALCO Center, Naperville, IL 60563.

<sup>§</sup> Permanent address: Institute of Physics, Jagellonian University, ul. Reymonta 4, PL-30059, Krakow 16, Poland.

<sup>⊗</sup> Abstract published in *Advance ACS Abstracts*, August 15, 1997.

(1) Allara, D. L.; Nuzzo, R. G. *Langmuir* **1985**, *1*, 45.

(2) Dubois, L. H.; Nuzzo, R. G. *Annu. Rev. Phys. Chem.* **1992**, *43*, 437.

(3) Lam, K. S. *Nature* **1991**, *352*, 82.

(4) Nuzzo, R. G.; Dubois, L. H.; Allara, D. L. *J. Am. Chem. Soc.* **1990**, *112*, 558.

(5) Ratner, B. D.; Boland, T.; Llanos, G.; Lewis, K. B.; Castner, D. G. *Polym. Mater. Sci. Eng.* **1992**, *66*, 220.

(6) Mrkisch, M.; Grunwell, J. R.; Whitesides, G. M. *J. Am. Chem. Soc.* **1995**, *117*, 12009.

(7) Cullision, J. K.; Hawkrige, F. M.; Nakashima, N.; Yoshikawa, S. *Langmuir* **1994**, *10*, 877.

(8) Madoz, J.; Kuznetsov, B. A.; Medrano, F. J.; Garcia, J. L.; Fernandez, V. M. *J. Am. Chem. Soc.* **1994**, *119*, 1043.

(9) Benninghoven, A.; Hagenhoff, B.; Niehuis, E. *Anal. Chem.* **1993**, *65*, 630A.

(10) Barber, M.; Bordoli, R. S.; Elliott, G.; Sedgwich, R. D.; Tyler, A. N. *Anal. Chem.* **1982**, *54*, 645A.

(11) Macfarlane, R. D.; Uemura, D.; Ueda, K.; Hirata, Y. *J. Am. Chem. Soc.* **1980**, *102*, 875.

(12) Hakansson, P.; Kamensky, B.; Sunqvist, B.; Fohlman, J.; Peterson, P.; McNeal, C. J.; Macfarlane, R. D. *J. Am. Chem. Soc.* **1982**, *104*, 2948.

(13) Hillenkamp, F.; Karas, M.; Beavis, R. C.; Chait, B. T. *Anal. Chem.* **1991**, *63*, 1193A.

(14) Winograd, N. *Anal. Chem.* **1993**, *65*, 622A.

(15) Mantus, D. S.; Ratner, B. D.; Carlson, B. A.; Moulder, J. F. *Anal. Chem.* **1993**, *65*, 1431.

(16) Muddiman, D. C.; Gusev, A. I.; Proctor, A.; Hercules, D. M.; Venkataramanan, R.; Diven, W. *Anal. Chem.* **1994**, *66*, 2362.

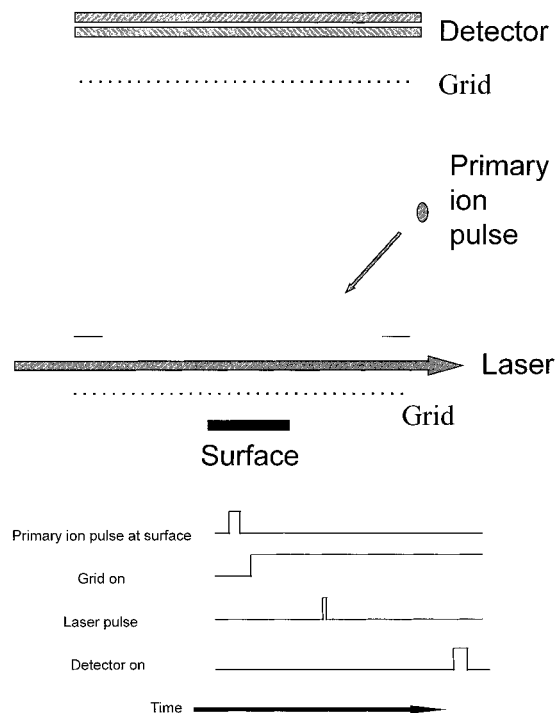


**Figure 1.** Experimental setup for collecting energy and angle-resolved neutral particle distributions.

### Experimental Section

Desorption from a self-assembled monolayer (SAM) of phenylethanethiol on gold was initiated by 8 keV, 500 ns pulses of  $\text{Ar}^+$  or  $\text{H}_2^+$  ions focused onto a 3 mm spot on the sample. Soon after ion impact an extraction field was applied to reject all sputtered ions. Ejected neutral molecules were detected by multiphoton ionization (MPI) using 266 nm, 6 ns, photon pulses (3 mJ/pulse) from a frequency quadrupled Spectra Physics GCR-5 Nd-YAG laser. The laser beam was focused to a ribbon shape parallel to the surface plane, located ca. 1 cm above the surface. Accurate surface to laser distance measurements were made using a telescope mounted on a micrometer before each experiment. A diagram of the apparatus is shown in Figure 1.

The density of molecules passing through the laser plane was recorded as a function of time by systematically varying the time delay between the primary ion and laser pulses.<sup>18</sup> This time delay corresponds to the flight time of the neutral molecule from the surface to the laser plane plus any measurable delay time to ejection from the surface. The photoionized neutral molecules were subsequently detected by time-of-flight (TOF) mass spectrometry using a gated position sensitive microchannel plate detector. The image was displayed on a phosphor screen and monitored by a charge-couple-device camera interfaced to a Pentium PC computer for data storage and processing. While this mode of operation enables accurate angular and time base measurements, the gated detector provides a mass resolution of approximately 20 at  $m/z$  100. Desorption profiles were obtained after averaging 100 laser shots at each delay time. The primary ion angle of incidence was 45°. The signal intensity normal to the surface was maximum, and the desorbed neutral molecules were monitored at 0° over an angular range of  $\pm 20^\circ$ . The desorption profiles were recorded by monitoring the intensity of ions falling in a time-gated mass window centered around  $m/z$  105. Ions falling in the  $m/z$  range 102–107 contribute to this signal under the ensuing conditions.

Measuring the time distributions of desorbed neutral molecules presents several experimental difficulties. First, translational energy determinations require accurate measurement of the distance between the surface and laser plane, and knowledge of the exact mass of the molecule. The fact that photofragmentation is likely to occur during

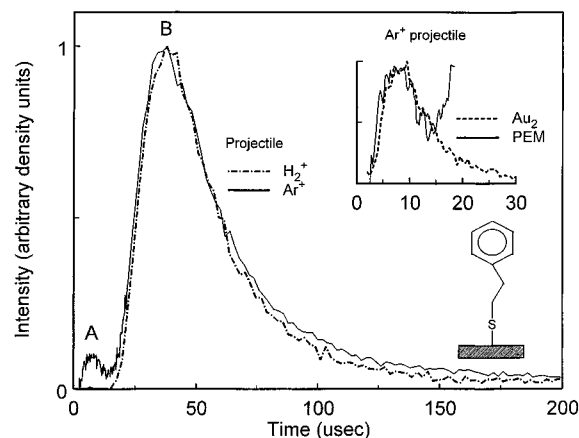


**Figure 2.** Time distributions for desorbed neutral molecules obtained using the  $\text{Ar}^+$  and  $\text{H}_2^+$  projectiles. The abscissa corresponds to the delay between the primary ion impact (time 0) and the ionizing laser pulse. The ordinate is the  $m/z$  105 photoion signal produced by the laser pulse and is proportional to the density of neutral molecules in the laser plane. See the text for details as to the neutral precursor of  $m/z$  105. The high and low translational energy components are labeled A and B, respectively. The high-energy component (peak A) is compared to the time distribution of sputtered  $\text{Au}_2$  (inset).

the ionization step leads to uncertainty in the identity of the desorbed neutral species. All fitting procedures and time–energy coordinate transformations were carried out by assuming 105 Da to be the mass of the desorbed neutral molecule. The implications of this assumption are discussed later. Second, time resolution increases as the distance between the surface and laser plane is increased but occurs with a corresponding decrease in signal intensity. Finally, the measurements must be made under static conditions in which damage inflicted to the surface over the course of the experiment is minimal. In our case, the total dose was kept below  $10^{10}$  incident ions/cm<sup>2</sup>.

Self-assembled monolayers were prepared by immersing vapor-deposited gold substrates in 30 mM solutions of phenylethanethiol in ethanol. The gold substrates were kept in solution for at least five days prior to use and were rinsed with ethanol before introduction into the UHV analysis chamber which had a base pressure of  $3 \times 10^{-10}$  Torr.

### Results and Discussion

**Projectile Dependence.** Room temperature desorption profiles for phenylethanethiol obtained using the  $\text{Ar}^+$  and  $\text{H}_2^+$  projectiles are shown in Figure 2. These distributions represent the time profile of the plume of neutral molecules passing through the laser plane. In general, the shapes of the profiles obtained using the two projectiles are similar. The maximum density of desorbed molecules passes through the laser plane approximately 40  $\mu\text{s}$  (peak B) after primary ion impact. An additional feature (peak A) is present in the profile produced by the  $\text{Ar}^+$  ion projectile. Upon performing the coordinate transformation to kinetic energy coordinates, it is found that peaks A and B correspond to approximately 1 and 0.03 eV, respectively.

**High-Energy Component.** The kinetic energies of the neutral molecules comprising peak A lie within the range usually observed for atoms sputtered from clean metal surfaces. Comparing the profiles of sputtered  $\text{Au}_2$  and phenylethanethiol upon bombardment with  $\text{Ar}^+$  ions (inset Figure 2) shows that these two species have nearly the same desorption profiles and hence leave the surface with the same velocity. This observation, along with the minimal intensity of both peak A and sputtered gold when using the lighter  $\text{H}_2^+$  projectile, indicates that this small, high-energy component is initiated by momentum transfer from the projectile to the gold substrate and finally to the organic layer.

(17) Brummel, C. L.; Lee, I. N. W.; Zhou, Y.; Benkovic, S. J.; Winograd, N. *Science* **1994**, *264*, 994.

(18) Kobrin, P. H.; Schick, G. A.; Baxter, J. P.; Winograd, N. *Rev. Sci. Instrum.* **1986**, *57*, 1354.

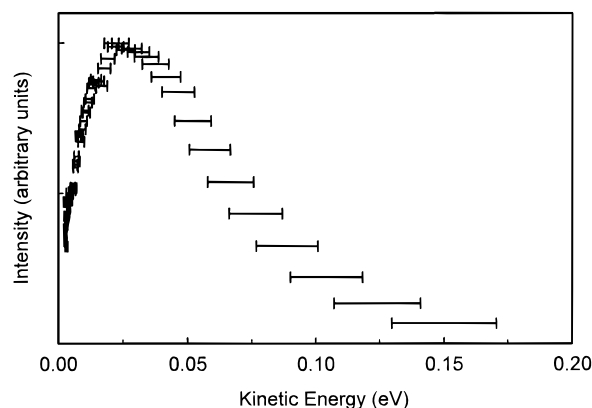


**Figure 3.** Translational energy distribution (flux) for desorbed neutral molecules calculated by transforming peak B (Figure 1). The width of the bar indicates the error introduced due to the uncertainty in the mass of the neutral precursor to  $m/z$  105 which is assumed to fall within the range  $m/z$  105–138.

The collision cascade model for atomic solids provides an analytical expression for kinetic energy distributions of sputtered atomic species.<sup>19,20</sup> Though it cannot be directly applied to molecular ejection, similarity between the energy distributions of substrate atoms and adsorbate molecules can be used to correlate the ejection of molecules to a ballistic process. Molecular dynamics simulations and experiments of kiloelectronvolt ion bombardment of  $C_6H_6/Ag\{111\}$  have shown that the kinetic energy distributions of the ejected neutral benzene and silver are similar.<sup>21</sup> Collisions originating in the silver substrate lead to the ejection of benzene molecules with energies around 1 eV. The ejection of phenylethanethiol molecules with energies around 1 eV (peak A, Figure 2) is due to a ballistic process.

**Low-Energy Component.** The low-energy component (peak B, Figure 2) is of particular interest since it indicates that most of the desorbed molecules leave the surface with extremely low translational energies. The corresponding translational energy distribution (Figure 3), which peaks near 0.03 eV, is indicative of equilibrated room temperature molecules and suggests that the translational energy of the molecules is dependent upon the macroscopic surface temperature. This is unexpected, especially when considering that desorption involves cleavage of a strong Au–S or S–C bond with an energy of 2–3 eV.<sup>22,23</sup> An initial conclusion is that the impact of kiloelectronvolt particles initiates a process which cleaves the surface linkage in a manner which is gentle enough to allow the nascent species to remain physisorbed and become thermally equilibrated with the substrate before desorbing. An additional point is that the shape and position of peak B are independent of projectile mass. This is strong evidence that momentum transfer via the gold substrate is not directly involved with the bond cleavage process. However, the signal produced by the  $Ar^+$  ion projectile was approximately 4 times greater than that produced by the  $H_2^+$  projectile, meaning energy deposited into the substrate may influence the yield of low-energy neutral molecules from the organic film via a secondary effect.

To help unravel the mechanisms involved, desorption profiles were recorded at different temperatures. Experimental distribu-

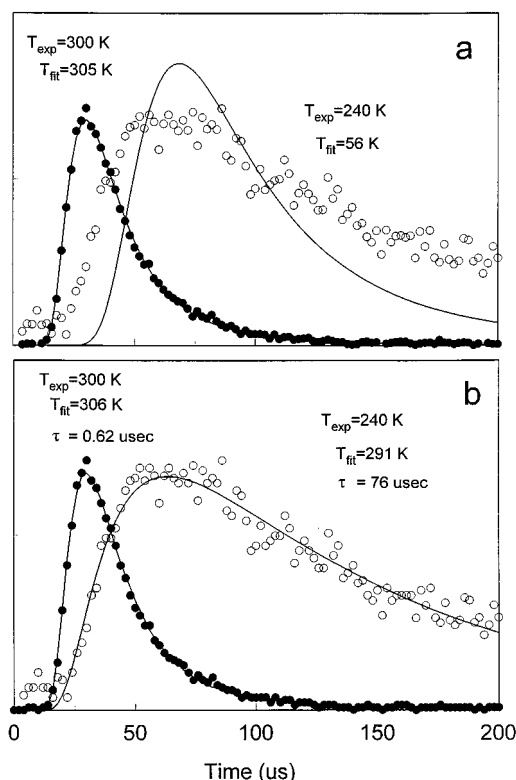


**Figure 4.** Time distributions (density) obtained at surface temperatures of 300 K (solid symbols) and 240 K (open symbols). The intensity of each distribution has been scaled to a maximum value of 1. The solid curves indicate the nonlinear least-squares fit with (a) a simple Maxwell–Boltzmann distribution (eq 1) and (b) the convolution of the Maxwell–Boltzmann distribution with the rate equation for first-order desorption (eq 2).

tions obtained at 300 and 240 K using the  $H_2^+$  projectile are plotted as points in Figure 4a. As the surface is cooled, the distribution broadens and shifts toward higher time. The same temperature dependent behavior was observed using the  $Ar^+$  ion projectile. The solid curves show the Maxwell–Boltzmann distribution (eq 1) which has been fit to the data at each

$$I(t) = Ct^{-4} \exp(-md^2/2ktT^2) \quad (1)$$

temperature using a nonlinear least-squares algorithm. The time–density form of the Maxwell–Boltzmann distribution is shown in eq 1 where  $m$  is the mass of the desorbed molecule,  $d$  is the distance from the surface to the laser plane,  $t$  is the delay between primary ion impact and the firing of the laser,  $T$  is the translational temperature of the desorbed molecules,  $k$  is the Boltzmann constant, and  $C$  is a proportionality constant. The room temperature data are fit well by this equation and yield a temperature parameter,  $T$ , of 305 K which agrees well with the experimental value of 300 K. However, the 240 K distribution is not well fit and yields an unreasonable temperature of 56 K. Hence, while the macroscopic surface temperature has a pronounced effect on the desorption profile, the shift toward higher time at lower temperatures cannot be explained solely on the basis of kinetic energy effects.

Further insights were made into this phenomenon by focusing on the experimental time variable which corresponds to the delay between the primary ion impact and laser pulse. If desorption is instantaneous, then the time delay corresponds to the flight time of an ejected neutral molecule from the surface to the laser. This assumption was used when fitting eq 1 to the data in Figure 4a. However, given the low kinetic energies observed at room temperature which point toward a thermal equilibrium process

(19) Thomson, M. W. *Philos. Mag.* **1968**, *18*, 377.

(20) Sigmund, P. *Phys. Rev.* **1969**, *184*, 383; **1969**, *187*, 768.

(21) Chatterjee, R.; Garrison, B. *J. Radiat. Eff. Defects Solids*, submitted for publication.

(22) Dubois, L. H.; Nuzzo, R. G. *Annu. Rev. Phys. Chem.* **1992**, *43*, 437.

(23) Lias, S. G.; Bartmess, J. E.; Liebman, J. F.; Holmes, J. L.; Levin, R. D.; Mallard, W. G. *J. Phys. Chem. Ref. Data* **1988**, *17*, Suppl. 1.

**Table 1.** Average of Six Fitted Values of  $T$  and  $\tau$  Obtained from Eq 2 at Each Surface Temperature<sup>30</sup>

| $T_{\text{exp}}$ (K) | av $T_{\text{fit}}$ (K) | $\sigma$ | av $\tau_{\text{fit}}$ ( $\mu\text{s}$ ) | $\sigma$ |
|----------------------|-------------------------|----------|--|----------|
| $300 \pm 3$          | 310                     | 17       | 0.42                                     | 0.2      |
| $270 \pm 5$          | 323                     | 18       | 20                                       | 3        |
| $240 \pm 10$         | 311                     | 50       | 76                                       | 16       |

prior to desorption, it is not unreasonable that desorption time delays may occur as the surface temperature decreases. Under low-temperature conditions, at any given time fewer molecules have enough kinetic energy to escape the surface potential well. Under these conditions desorption is viewed as a process described by first-order kinetics with a rate that is dependent on the surface temperature. Upon desorption, the molecule will traverse the distance from the surface to the laser with a kinetic energy that is related to the surface temperature.

This model was applied by altering eq 1 to include a desorption delay term. This form corresponds to a convolution of the Boltzmann distribution with the first-order rate equation as shown in eq 2 where  $t$  is the delay between primary ion

$$I(t) = C \int_{t'=0}^t [(t-t')^{-4} \exp(-ma^2/2kT(t-t')^2)] \exp(-t'/\tau) dt' \quad (2)$$

impact and the firing of the laser,  $t'$  is the desorption delay,  $T$  is the translational temperature of the desorbed molecules, and  $\tau$  is the mean delay to desorption. This equation was fit to the experimental data by allowing adjustment of  $C$ ,  $T$ , and  $\tau$ . A resulting fit obtained at 300 and 240 K is displayed in Figure 4b. Note that eq 2 provides a good fit to the experimental data at both room temperature and when the substrate is cooled. Desorption profiles were obtained at three surface temperatures and at six different sample-to-laser distances. Each distribution was well fit by eq 2, and the average fitted values of  $T$  and  $\tau$  obtained at each surface temperature are shown in Table 1.

At 300 K there is almost no measurable delay to desorption,  $\tau < 1 \mu\text{s}$  (Table 1). This is in agreement with the fact that the data obtained at this surface temperature are also well fit by a simple Boltzmann (eq 1) with no delay term (Figure 4a). As the sample is cooled there is a marked increase in the delay to desorption. When the substrate is cooled to 270 K, the average desorption delay time is 20  $\mu\text{s}$ , and this delay increases to 76  $\mu\text{s}$  upon further cooling to 240 K. The fitted values for  $T$  (Table 1) indicate there is no discernible change in the translational temperature of the molecules over the temperature range investigated. Specifically, an expected trend toward lower translational energy at lower surface temperature is not observed. Note, however, that a change in translational temperature from 300 to 240 K corresponds to a change of only 0.002 eV in the mean Maxwell-Boltzmann translational energy and a corresponding shift of only 6  $\mu\text{s}$  in the time distribution. In addition, the uncertainty in the fitted  $T$  values increases as the surface temperature decreases (Table 1) due to a lower signal-to-noise ratio. It is believed that these factors preclude the observation of a small kinetic energy shift over the narrow temperature range investigated.

**Considerations Pertaining to the Mass of the Ejected Neutral Molecules.** Fitting the Maxwell-Boltzmann equation to the data requires knowledge of the mass of the neutral molecular species desorbed from the surface. Some uncertainty is introduced by monitoring the ion signal in a 5 Da window centered around  $m/z$  105. The fact that photofragmentation may occur during the ionization step introduces additional uncertainty as to the exact mass and identity of the desorbed species. It is possible that ions in the window around  $m/z$  105 originate

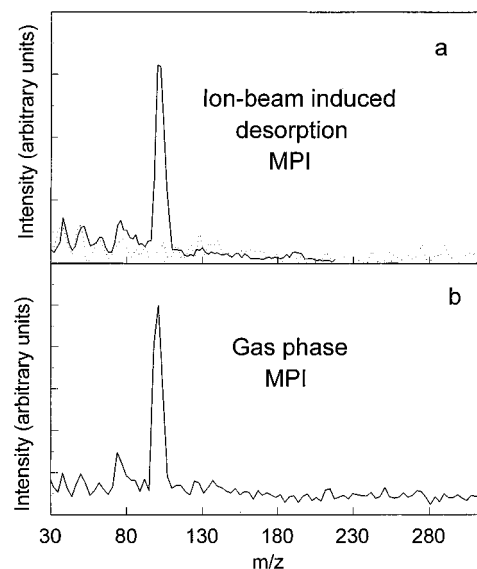


**Figure 5.** MPI mass spectra using a focused 266 nm laser beam (3 mJ/pulse). Spectrum a displays the laser-ionized neutral molecules desorbed by the pulsed ion beam (solid line). A background scan (dotted line) obtained in the absence of the pulsed ion beam is also shown. Spectrum b shows the gas phase MPI spectrum of phenylethanethiol introduced into the chamber to obtain a pressure of  $1 \times 10^{-9}$  Torr.

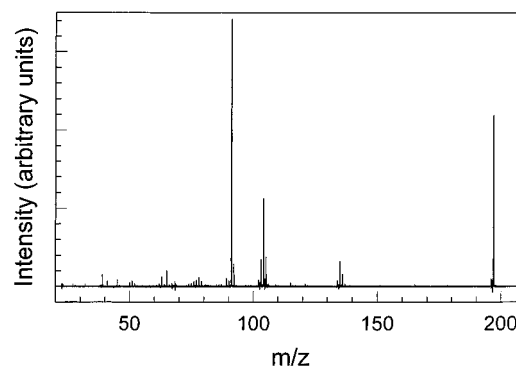


**Figure 6.** MPI mass spectrum of neutral molecules after desorption by 30 keV  $\text{Ga}^+$  projectile ions and ionization by a 266 nm, 300 fs laser pulse at a laser intensity of  $1.88 \times 10^{10}$  W/cm<sup>2</sup>.

from a larger neutral precursor (e.g.,  $\text{C}_6\text{H}_5\text{CH}_2\text{CH}_2\text{S}^*$  or  $\text{C}_6\text{H}_5\text{CH}_2\text{CH}_2\text{SH}$ ) and that photofragmentation to form the detected lower mass species occurs during the ionization process. It is also possible that neutral molecules of  $m/z \sim 105$  may be emitted directly from the surface, or that both scenarios may contribute to the detected signal near  $m/z$  105. No molecular ion was observed in the postionization mass spectrum even at near threshold laser power, and a nearly identical spectrum was obtained from multiphoton ionization of gaseous phenylethanethiol (Figure 5), although shifts of  $\pm 1$  Da would not be detected under the ensuing low-resolution condition. This indicates that if the desorbed neutral molecule is phenylethanethiol, then it would be detected as  $m/z$  105, but does not rule out the possibility that a molecule having a  $m/z$  near 105 is emitted directly from the surface.

Additional experiments were performed in which neutral molecules ejected from this surface were ionized by femtosecond 266 nm radiation pulses in a high-resolution reflectron time-of-flight instrument (Figure 6). In this experiment desorption was initiated by 30 keV  $\text{Ga}^+$  ions. This spectrum differs significantly from the one obtained using the nanosecond laser, although this is not unexpected given the dramatic differences often observed between nanosecond and femtosecond ionization

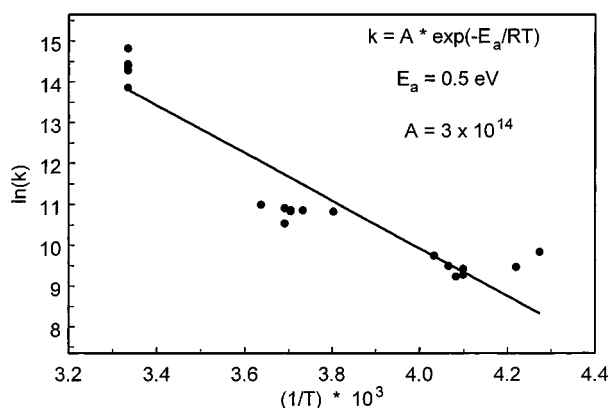


**Figure 7.** An Arrhenius plot of the experimental points and best fit line. Values for  $k$  were determined from the mean delay times using eqs 2 and 3.

processes.<sup>24</sup> The use of  $\text{Ga}^+$  ions in place of  $\text{Ar}^+$  ions is not expected to strongly influence the observed result. An important feature is the presence of an ion at  $m/z$  135. The presence of this ion indicates that intact molecular or pseudomolecular thiolate species are ejected from the surface as neutral molecules upon high-energy ion bombardment. Prominent ions also appear at  $m/z$  104 and 91, but it is not possible to ascertain whether or not photofragmentation is involved in their formation. The peak at  $m/z$  197 is from ejected neutral gold atoms which are readily photoionized.

As mentioned above all coordinate transformations and curve-fitting procedures were carried out assuming  $m/z$  105 to be the mass of the neutral precursor. The fact that at least some the desorbed neutral molecules have masses near  $m/z$  135 will introduce some error into the translational energy measurements. Maximum error will occur if all of the ejected neutral molecules had masses in the range  $m/z$  135–138. This worst case condition would increase the fitted Boltzmann temperatures by approximately 90 K, yielding translational temperatures of about 400 K. However, it is important to realize that the fitted value of  $\tau$  is not affected by the mass of the ejected molecule, and the desorption delay is not influenced by this uncertainty in the mass of the neutral molecule.

**Temperature Dependent Desorption Rate.** Of primary significance is that most of the change in the profiles as a function of temperature is due to the desorption delay. Since the rate constant,  $k$ , for the desorption process is the reciprocal of the  $\tau$  parameter (eq 3), the activation energy,  $E_a$ , can be

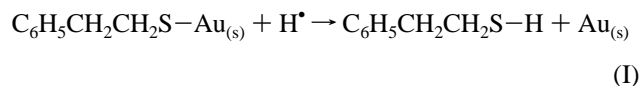
$$k = 1/\tau \quad (3)$$

determined using the Arrhenius equation. The corresponding plot, which is displayed in Figure 7, yields a binding energy of 0.5 eV which is in the range expected for physisorbed organic molecules on metal surfaces.<sup>25,26</sup> A value of  $\sim 3 \times 10^{14}$  was obtained for the preexponential factor and is consistent with a first-order process.

All of these features are characteristic of thermalized molecules evaporating from a surface. An ensuing picture is that desorption occurs via a two-step process consisting of (i) cleavage of an adsorbate–surface bond or a bond within the adsorbate and (ii) surface trapping (physisorption) which eventually leads to evaporation of the thermally equilibrated

molecules. The nascent physisorbed molecules desorb from the surface with a Maxwell–Boltzmann translational energy distribution and at a rate which depends on the temperature of the surface.

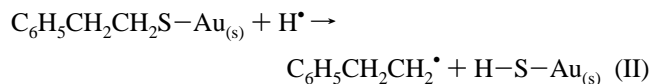
**Cleaving the Covalent Surface Linkage.** An unanswered question is how the impact of a high-energy primary ion breaks the adsorbate–substrate bond in a manner gentle enough to allow the nascent molecule to remain trapped at the surface. Direct bond scission, initiated by a ballistic interaction or another process, is unlikely since such an event would inevitably impart energies significantly greater than the bond energy and result in immediate desorption at nonthermal energies. While the process responsible for cleavage of the S–Au or C–S adsorbate–surface bond warrants further investigation, a mechanism consistent with the above observations is cleavage by a chemical reaction. Many of the surface molecules near the primary ion impact zone will be severely damaged and yield highly reactive species such as  $\text{H}^\bullet$  and other ionic or neutral molecular fragments.<sup>27</sup> It is feasible that these unstable species may react with intact molecules and sever the surface bond. Bond cleavage by reaction should be more gentle than direct bond scission and is more likely to form low translational energy products which may be trapped at the surface. A possible scenario is shown in reaction I. Direct scission of the sulfur–



gold bond is endothermic by approximately 2 eV,<sup>22</sup> while cleavage by reaction with a hydrogen radical is estimated to be exothermic by 1.7 eV.<sup>28</sup>

Several factors should be reemphasized here. As mentioned above, the neutral precursor(s) to the  $m/z$  105 ion, used to record the time profiles, is not known since photofragmentation of possible larger neutral molecules to form  $m/z$  105 is possible. Reasonable candidates are  $\text{C}_6\text{H}_5\text{CH}_2\text{CH}_2^\bullet$  ( $m/z$  105),  $\text{C}_6\text{H}_5\text{CH}_2\text{CH}_2\text{S}$  ( $m/z$  137),  $\text{C}_6\text{H}_5\text{CH}_2\text{CH}_2\text{S}-\text{H}$  ( $m/z$  138), or larger species of the form  $\text{C}_6\text{H}_5\text{CH}_2\text{CH}_2\text{S}-\text{R}$ . Not knowing the specific identity of the neutral species precludes postulation of a chemically specific reaction mechanism. However, regardless of the specific identity of the neutral precursor to  $m/z$  105, the observation of near thermal translational energies and delayed ejection make a violent direct bond scission unlikely. Bond cleavage by a surface reaction is a more likely alternative which is consistent with the observed behavior.

While the occurrence of a reaction is unproven, several factors are in accord with this or a similar process. First, the cleavage by a reaction is energetically favorable. Although such reactions may have exothermicities which are on the order of the surface binding energy of the nascent physisorbed species, this should not preclude surface trapping since the excess energy is distributed between translational and internal modes. Note that a larger precursor is not a necessity for reaction. For example, we do not rule out the occurrence of reaction II or other similar



processes. Second, the release of bound surface molecules by reaction with hydrogen radicals produced from nearby damaged surface molecules has been observed in molecular dynamics

(24) Weinkauff, R.; Aicher, P.; Wesley, G.; Grottemeyer, J.; Schlag, E. *J. Phys. Chem.* **1994**, *98*, 8381.

(25) Xi, M.; Yang, M. X.; Jo, S. K.; Bent, B. E. *J. Chem. Phys.* **1994**, *101*, 9122.

(26) Dubois, L. H.; Zegarski, B. R.; Nuzzo, R. G. *J. Chem. Phys.* **1993**, *98*, 678.

(27) Taylor, R. S.; Garrison, B. J. *Langmuir* **1995**, *11*, 1220.

(28)  $\Delta H_{\text{rxn}}$  was calculated using the following parameters:  $D(\text{RS}-\text{Au}(s)) = 2$  eV (ref 22);  $D(\text{RS}-\text{H}) = 3.7$  eV which is  $\Delta H_{\text{rxn}}$  for the process  $\text{CH}_3\text{SH} \rightarrow \text{CH}_3\text{S}^\bullet + \text{H}^\bullet$  (ref 23).

simulations.<sup>27</sup> In addition, reactions between low-energy ions and adsorbate molecules often result in the abstraction of covalently bound surface species.<sup>29</sup> Finally, the 4-fold increase in signal observed using Ar<sup>+</sup> ions as a primary ion is in accord with such a mechanism since the increased energy deposited into the substrate by this heavier projectile will likely induce additional damage to the molecular overlayer and thereby increase the number of reactive precursors.

### Conclusion

The time dependent desorption profiles of ion-beam-desorbed neutral molecules from a self-assembled monolayer of phenylethanethiol have been measured subsequent to 8 keV ion bombardment. The effect of projectile mass has been used to separate ballistic and thermal desorption processes. While a minor collision-induced ejection is observed only with the heavier Ar<sup>+</sup> primary ion, most molecules desorb with very low thermal kinetic energies using both Ar<sup>+</sup> and much lighter H<sub>2</sub><sup>+</sup>

(29) Cooks, R. G.; Ast, T.; Pradeep, T.; Wysocki, V. H. *Acc. Chem. Res.* **1994**, *27*, 316.

(30) Displayed are the average values of  $T_{\text{fit}}$  and  $\tau_{\text{fit}}$ , and their respective standard deviations obtained from nonlinear least-square fits of eq 2 to six experimental time distributions at each temperature.  $T_{\text{exp}}$  is the experimentally measured surface temperature. Uncertainties ( $\pm$ ) in  $T_{\text{exp}}$  values reflect limitations in the precision with which experimental surface temperatures could be reproduced during sequential runs.

ion projectiles. The temperature dependent desorption profiles of the low kinetic energy component are well fit by a convolution of the Maxwell–Boltzmann distribution with the rate equation for first-order desorption. The results implicate a two-step desorption mechanism consisting of (i) breakage of the covalent surface linkage followed by (ii) thermal equilibration and evaporation. A mechanism has been suggested for gentle cleavage of the surface linkage. This proposed mechanism involves a reaction between the adsorbate and radicals or other high-energy species formed during the bombardment process. The existence of such a mechanism would provide a partial explanation for the fact that the yield of neutral molecules often greatly exceeds the yield of ions and reemphasizes the importance of utilizing laser techniques for detection of these neutral surface species.

**Acknowledgment.** The financial support of the National Science Foundation, the National Institutes of Health, the Office of Naval Research, and the Polish Committee for Scientific Research Fund No. PB 1128/T08/96/11 are gratefully acknowledged. K. F. Willey, C. L. Brummel, and B. J. Garrison are acknowledged for numerous useful discussions. K. F. Willey and R. M. Braun are thanked for the femtosecond laser experiment.

JA971083V